Minimal variation in eutherian brain growth rates during fetal neurogenesis
Andrew C Halley
Proceedings of the Royal Society B: Biological Sciences
doi:10.1098/rspb
Supplementary Material

1. Dataset collection

Data on the weight of fetal brain, body, heart, liver, lung (x2), and kidney (x2), as well as post-conception age in days were collected from published literature. Data sources were identified from searching online databases for keywords (e.g. "brain," "growth," "fetal"), from previous studies of brain growth, and from searching journals in which original data is frequently published. Data were excluded from this study if sources (a) included visceral organ, but not brain growth data; (b) only included postnatal brain growth data; (c) did not exhibit a clear sigmoid curve in brain growth (i.e. did not include exponential portions of brain growth); or (d) did not include data distributed over ontogeny, as required for model fitting. In the case of experimental studies, only data from healthy control animals was included. When individual observations were not published in the original paper, data were reconstructed from figures using Photoshop CC and are labeled as such in the corresponding tables below. Most observations represent average values as originally published.

Data on neonatal brain and body size in the ten eutherian mammals described in this paper are taken from the following sources: human (Sacher & Staffeldt, 1974); macaque (Kerr et al., 1974); marmoset (Sacher & Staffeldt, 1974); pig (Ullrey et al., 1965); sheep (Sacher & Staffeldt, 1974); ox (Sacher & Staffeldt, 1974); rabbit (Edson et al., 1975); guinea pig (Edwards et al., 1976); mouse (Wingert, 1969); rat (Sikov & Thomas, 1970; 21dg average). All other species' data on neonatal brain size, as well as gestation length for all species, is taken from Sacher & Staffeldt (1974) and Harvey & Clutton-Brock (1985). Age estimates for Carnegie Stage 10 was taken from sources listed in Figures S6-S15.

2. Gompertz & velocity models

For any given species and organ, individual studies differ systematically in age estimation, as reflected in intercept shifts in cube root models below. Accordingly, Gompertz models are best fit to brain growth data using a subset of datasets rather than pooling all available data. Sources used to fit Gompertz models are listed separately from subsequent cube-root model sources (Figs. S6-15), which were fit to larger numbers of published datasets. Gompertz models were fit to fetal, perinatal, and early postnatal data to improve model fit; as such, asymptotes do not reflect adult brain size, and velocity curves are only approximate. The primary function of growth models was to estimate the timing of peak velocity in a non-biased way in order to isolate exponential data for cube-root modeling.

Gompertz models were autofit to brain growth data using nonlinear least squares curve fitting with the nls function in the {stats} package for R. Velocity functions were calculated from the first order derivative of the Gompertz model. The age of neurodevelopmental events in available species were taken from models developed from empirical data (Workman et al., 2013) and available on the Translating Time website (translatingtime.net). Events were coded as involving neurogenesis, tract formation, or myelination and fit to velocity curves in available species.

3. Cube Root Models

Brain growth data preceding peak velocity, as calculated from Gompertz autofit functions, were considered exponential and were included in cube root models. In species born earlier than peak velocity, all exponential data (including early postnatal data) were included in this analysis. Whole body growth data includes all fetal data in each species, as body growth peak velocity is always postnatal. Exponential growth data for liver, heart, lungs, and kidneys were isolated by visually inspecting cube-root data, determining a point of growth deceleration, and removing values older that.

Cube root models were calculated separately by data source for each organ and species to minimize artifacts introduced from differences in age estimation across studies (i.e. intercept shifts; see cube root models below). Exponential data from each study was cube-root transformed, and ordinary least squares (OLS) models were fit predicting cube-root weight in grams from days post-conception. Model parameters were then averaged across available studies to produce a final slope estimate for statistical tests (Table S1).

4. Instantaneous growth rate calculation

Data preceding peak velocity, as calculated in Gompertz models (see Figs. S6-S16), are included for each species. Instantaneous velocities (g/d) were calculated by taking the slope between adjacent data points according to increasing age (i.e. $(mass_2 - mass_1)/(age_2 - age_1)$). As sources differ in post-conceptual age approximation, reflected as intercept shifts along cube-root models (Figs. S6-S16), velocities were calculated separately by source. Data was averaged by day post-conception in mouse (Goebloed, 1976; Wingert, 1969) and rat (Goedbloed, 1976) to allow velocity calculation between time periods.

Instantaneous velocity calculated from raw data regularly indicates unlikely values, such as sudden decreases in velocity (i.e. negative values) or abnormally high or low velocities at a given brain size, often caused by data clustering over short age intervals (e.g. the smallest brain sizes)(Fig. S1c). Negative velocities were removed from the sample. To remove remaining outlier values, ordinary least-squares regression models were fit to velocities according to brain size in log-log coordinates for each individual species subsample. Values outside of the 95% confidence interval were removed (they are included in the Supporting Data and labeled as outside the 95% CI). The remaining data for each species are included in subsample regressions depicted in Figure 3.

5. Altricial vs. precocial species.

Variation in birth timing affects any analysis of neonatal brain size (raw, exponential, or allometric), and is well demonstrated by unpacking two conflicting findings in the literature. Using cube-root models, Sacher & Staffeldt (1974) noted that altricial species achieve similar neonatal brain sizes to precocial species over shorter gestation periods, implying faster altricial brain growth. In contrast, Barton & Capellini (2011) found that altricial species have smaller brains once gestation length is corrected for (implying faster precocial growth). These studies use the same variables (neonatal brain size and gestation length) and similar datasets, but arrive at opposite conclusions – why?

The current study clearly demonstrates that altricial species are born during growth acceleration, while precocial species are born during the decay curve (Fig. 4). Sacher & Staffeldt's technique artificially depresses acceleration estimates in precocial species by applying exponential (cubic) models to non-exponential data (i.e. portions of the decay curve; red dotted line in Fig. S2d), producing the birth timing artifact described in the introduction. Conflicting evidence for precocial acceleration comes Barton & Capellini, who predict raw neonatal brain size from altriciality/precociality, correcting for gestation length. This treats fetal brain growth as linear, which nearly always produces higher estimates for species born later during sigmoid brain growth, namely precocial species with small litter size (Fig. S2d).

The present study does not support either theory, and suggests that altricial and preococial species exhibit similar brain acceleration in utero. We agree that precocial and altricial species vary regularly in both neonatal brain size vs. gestation length, as well as neonatal brain/body proportions vs. gestation length. However, this variation is a consequence of birth timing relative to brain and brain/body growth patterns, respectively.

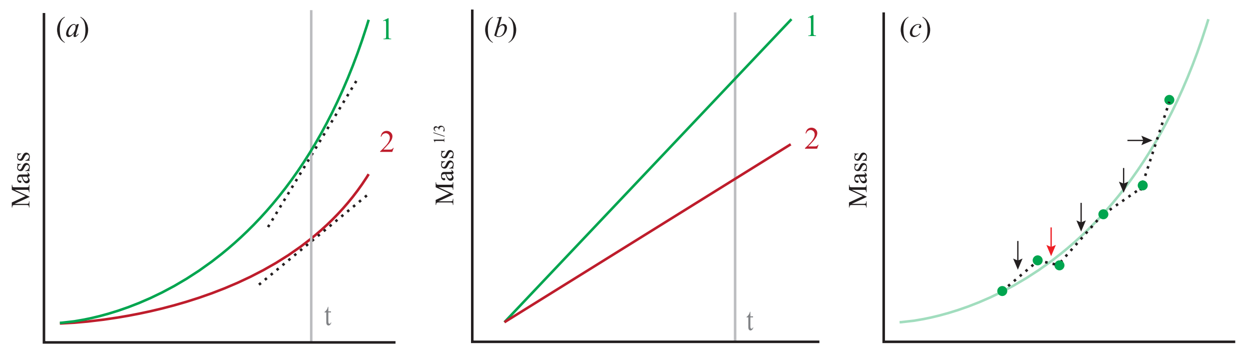

Figure S1. Models of exponential growth using a set exponent, traditionally cubic, can be used to compare growth acceleration using a single variable, slope. (*a*) Two cubic functions with higher (1) and lower (2) coefficients differ in mass size and growth velocity (dotted line) at any given time (t) following an identical onset of exponential growth. (*b*) Linear models predicting cube-root transformed mass show differences in slope, corresponding to the relative acceleration rate of brain growth in species 1. (*c*) Instantaneous velocity can also be calculated directly from raw data by taking the slope between two points (dotted lines) and assigning it to average brain mass or age. However, this method produces artifacts (red arrow), particularly in clustered data.

Figure S2. Birth timing artifacts in neonatal brain size

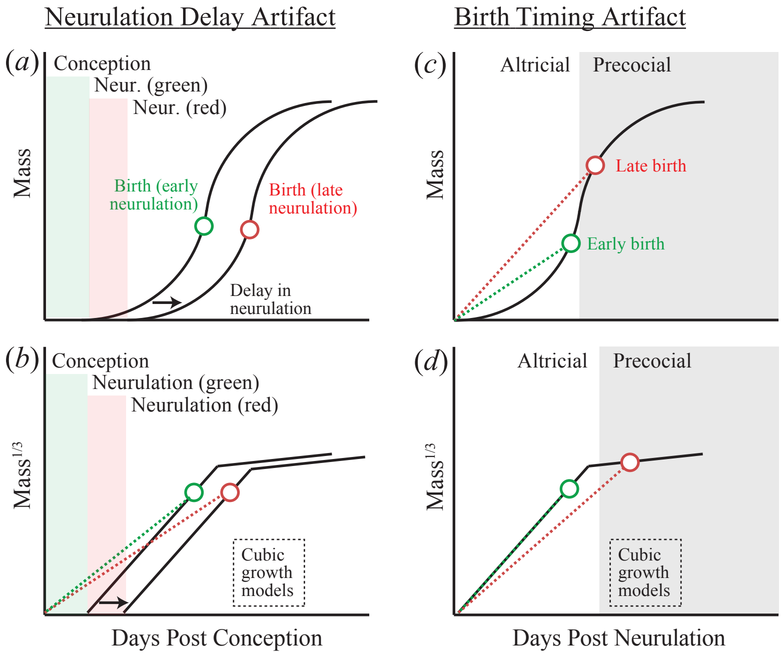

Figure S3. Birth timing artifacts in allometric growth (unknown age)

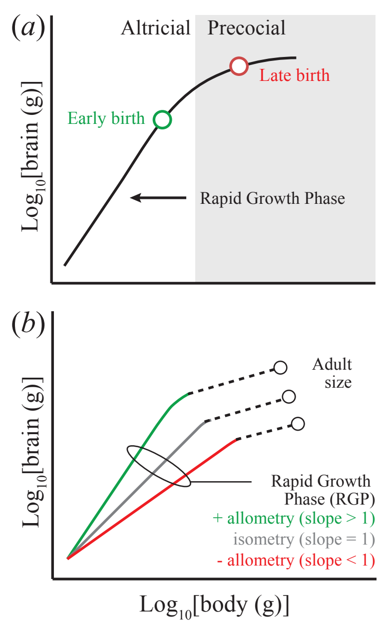

Figure S2. Several artifacts complicate the interpretation of neonatal brain size. (*a*) First, species differ in the elapsed time from conception to the formation of the neural tube and the onset of brain growth. Here, two idealized species exhibit identical sigmoid brain growth patterns, but differ in the duration of pre-neurulation embryogenesis. (*b*) Cube root models of neonatal brain size vs. total gestation length (dotted lines) are artificially depressed compared to actual growth patterns (solid black lines) by including this early period. Species with longer delays in neurulation (red) are more strongly affected by this artifact when compared with species with shorter delays (green). (*c*) In addition to the neurulation artifact, differences in birth timing produce regular variation in neonatal values. Here, two idealized species exhibit the same neurulation delay and the same brain growth pattern, but are born along differing portions along the brain growth curve. Linear models (dotted lines) are produced by predicting raw neonatal brain size from gestation length, giving an average mass/day for all of gestation. This measure is heavily influenced by differences in birth timing, and is uncorrelated to brain growth acceleration in this study. (*d*) Cube root models from neonatal values (dotted lines) artificially depress slope estimates in precocial species. Both the neurulation and birth timing artifacts are removed in the current dataset by isolating exponential data and focusing on slope over intercept, respectively.

Figure S3. Over ontogeny, brain/body proportions change in a regular way in any given species. (*a*) In log-log coordinates, fetal development is characterized by a roughly linear period of exponential brain and body growth - the Rapid Growth Phase (RGP; Renfree et al. 1982). Species born earlier along an allometric trajectory - e.g. altricial species in large litters - exhibit higher brain/body proportions at birth. (*b*) Species differ in the slope of the RGP (Halley, 2016), with higher slopes signifying either faster brain or slower body growth. The current study suggests that higher RGP slopes are caused by slower body growth.

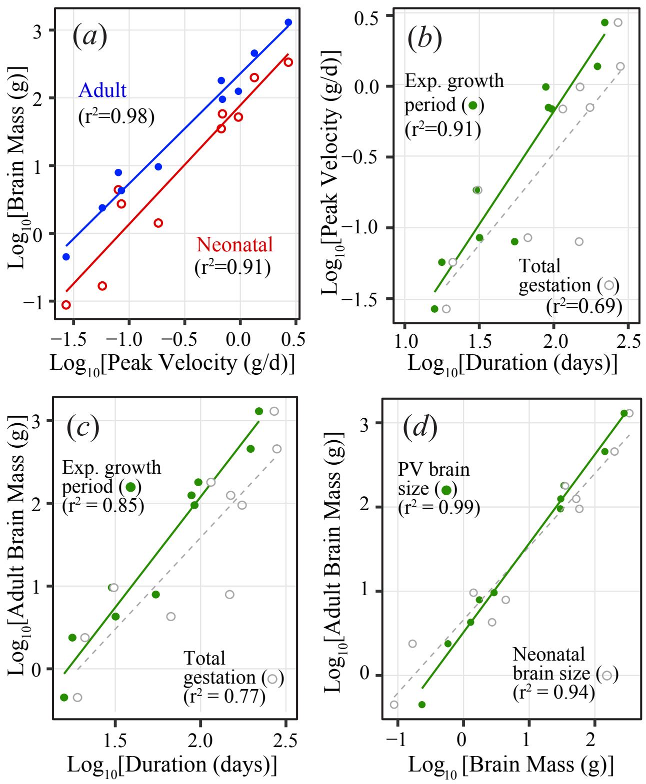

Figure S4. (*a*) Peak brain velocity (g/d) predicts adult brain size (blue) better than neonatal brain size (red), as might be expected from variation in birth timing. (*b*) The age of peak velocity (green) predicts peak velocity better than total gestation length (grey). (*c*) Age of peak velocity (green) is similarly a better predictor of adult brain size than is total gestation length (grey). (*d*) Brain size at peak velocity (green) is a better predictor of adult brain size than neonatal brain size (grey). Together, this indicates that peak brain growth velocity and its associated brain size is more closely linked to underlying neurodevelopment and adult phenotypes than is neonatal brain size.

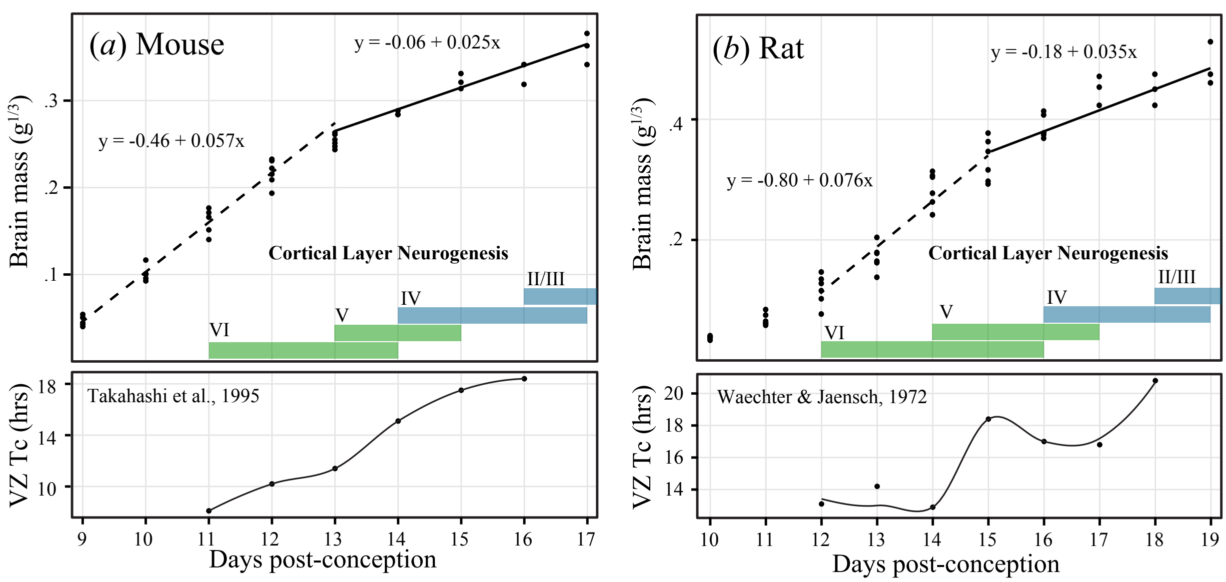

Figure S5. Embryonic brain growth in (*a*) mouse and (*b*) rat from Goedbloed (1976) shows more rapid acceleration prior to E13 and E15, respectively. Color bars indicate windows of cortical neurogenesis by layer, taken from neurodevelopmental event models (Workman et al., 2013). Below, cell cycle duration (Tc) in the ventricular zone (VZ) of each species increases as larger proportions of progenitors enter neurogenic (asymmetric) division. Whole brain growth rates decelerate and cell cycle duration increases sharply around the onset of layer IV neurogenesis, which is thought to coincide with the contraction of the symmetrically dividing progenitor pool (Caviness et al., 1995).

Table S1. Organ slope averages

Average slope values from brain (Figures S6 – S17), whole body (Table S8; Figure S18) and visceral organ (Tables S9-S10; Figures S19-S22) OLS models predicting (brain mass)$^{1/3}$ from days post-conception.

	Body	*Brain*	*Liver*	*Heart*	*Lungs*	*Kidneys*
Homo sapiens	0.0654	0.0326	0.0230	0.0128	0.0175	0.0141
Macaca mulatta	0.0648	0.0331	0.0231	0.0114	0.0179	0.0125
Callithrix jacchus	0.0350	0.0235	0.0132	0.0125	0.0157	0.0074
Ovis aries	0.1687	0.0387	0.0514	0.0316	0.0552	0.0278
Sus scrofa	0.1027	0.0371	0.0270	0.0200	0.0330	0.0201
Bos taurus	0.1441	0.0220	0.0334	0.0297	0.0368	0.0172
Orycto. cuniculus	0.1803	0.0473	0.0917	0.0434	0.0517	0.0493
Cavia porcellus	0.0887	0.0316	0.0296	0.0151	0.0295	0.0194
Mus musculus	0.1019	0.0250	0.0555	0.0157		0.0225
Rattus rattus	0.1616	0.0356	0.0768	0.0335	0.0621	0.0356
Euth. var. (x1000)	**2.4925**	**0.0597**	**0.6608**	**0.1240**	**0.3035**	**0.1508**
Macropus eugenii		0.0123				
Monodelphis dom.		0.0133				
C. virgianus		0.0416				
M. undulates		0.0345				

Table S2. Organ variance F tests.

Comparison of variance in average slope values for brain vs. whole body, liver, heart, lungs, and kidneys. Values are given for the whole eutherian sample (n=10).

vs. Brain	*F stat.*	*df*	*p*	
Body	41.74	(9,9)	0.000	***
Liver	11.07	(9,9)	0.001	**
Heart	2.08	(9,9)	0.292	
Lungs	5.08	(8,9)	0.025	*
Kidneys	2.53	(9,9)	0.184	

Table S3. Organ slope correlation table

	Total eutherian sample (n=10)				
	Brain	*Liver*	*Heart*	*Lungs*	*Kidneys*
Body	0.545	0.837**	0.945***	0.943***	0.857**
Brain		0.602	0.584	0.550	0.755*
Liver			0.840**	0.872**	0.964***
Heart				0.960***	0.899**
Lungs					0.823*

Table S4. OLS organ slope regression models

EV: Body cube root slope	slope	int.	*t*	*p*	df	r^2	*sig.*
Brain cube root slope	0.084	0.023	1.84	0.103	8	0.30	ns
Liver cube root slope	0.431	-0.006	4.33	0.003	8	0.70	**
Heart cube root slope	0.211	-0.001	8.17	0.000	8	0.89	***
Lungs cube root slope	0.311	0.001	7.51	0.000	8	0.89	***
Kidneys cube root slope	0.211	-0.001	4.70	0.002	8	0.73	**

Table S5. OLS bivariate regression models

Dependent variable *Explanatory variable*	slope	int.	*t*	*p*	df	r^2	*sig.*
Log^{10}(adult brain [g])							
Log^{10}(peak velocity [g/d])	1.63	2.36	17.85	0.000	8	0.98	***
Log^{10}(gestation [d])	2.21	-2.84	5.15	0.001	8	0.87	***
Log^{10}(PV age [d])	2.91	-4.01	6.73	0.000	8	0.95	***
Log^{10}(neo brain [g])	0.87	0.66	11.41	0.000	8	0.94	***
Log^{10}(PV brain [g])	1.06	0.51	28.04	0.000	8	0.99	***
Log^{10}(neo. brain [g])							
Log^{10}(peak velocity [g/d])	1.76	1.89	9.16	0.000	8	0.91	***
Log^{10}(gestation [d])	0.01	-0.59	6.39	0.000	8	0.84	***
Log^{10}(PV age [d])	0.01	-0.56	5.30	0.000	8	0.78	***
Peak brain velocity (g/d)							
PV age (d)	0.01	-0.35	5.84	0.000	8	0.81	***
Brain cube root slope							
Placental type (dummy)	0.00	0.03	0.01	0.991	8	0.00	ns
Relative BMR	0.03	-0.00	-0.75	0.476	8	0.07	ns
Altricial/precocial (dummy)	0.00	0.04	-0.84	0.407	8	0.09	ns
Neonatal brain/body ratio							
Brain cube root slope	-2.33	0.13	-1.14	0.287	8	0.14	ns
Body cube root slope	-0.80	0.15	-4.26	0.003	8	0.69	**
Allometric RGP slope							
Brain cube root slope	-5.13	1.03	-1.01	0.348	7	0.13	ns
Body cube root slope	-2.03	1.10	-5.33	0.001	7	0.80	**

Table S6. PGLS organ slope regression models

Phylogenetic generalized least squares (PGLS) regressions were performed on all statistical tests described in Tables S4-S5. A mammalian supertree (Bininda-Emonds) was downloaded and pruned to the ten eutherian species described here using the {ape} package in R. PGLS models were performed using the {caper} package.

EV: Body cube root slope	slope	int.	*t*	*p*	df	r^2	*sig.*
Brain cube root slope	0.141	0.018	2.41	0.043	8	0.42	*
Liver cube root slope	0.459	-0.008	5.55	0.001	8	0.79	***
Heart cube root slope	0.227	-0.002	7.25	0.000	8	0.87	***
Lungs cube root slope	0.322	0.000	5.56	0.001	8	0.82	***
Kidneys cube root slope	0.234	-0.003	5.70	0.000	8	0.80	***

Table S7. PGLS bivariate regression models

Dependent variable *Explanatory variable*	slope	int.	*t*	*p*	df	r^2	*sig.*
Log^{10}(adult brain [g])							
Log^{10}(peak velocity [g/d])	1.61	2.35	12.37	0.000	8	0.95	***
Log^{10}(gestation [d])	2.32	-3.04	3.51	0.008	8	0.61	**
Log^{10}(PV age [d])	2.90	-4.03	4.78	0.001	8	0.74	**
Log^{10}(neo brain [g])	0.95	0.59	8.38	0.000	8	0.90	***
Log^{10}(PV brain [g])	1.05	0.53	17.54	0.000	8	0.97	***
Log^{10}(neo. brain [g])							
Log^{10}(peak velocity [g/d])	1.53	1.75	7.19	0.000	8	0.87	***
Log^{10}(gestation [d])	2.69	-4.29	6.13	0.000	8	0.82	***
Log^{10}(PV age [d])	3.03	-4.83	6.07	0.000	8	0.82	***
Peak brain velocity (g/d)							
PV age (d)	0.01	-0.38	4.66	0.002	8	0.73	**
Brain cube root slope							
Placental type (dummy)	0.00	0.03	-0.04	0.967	8	0.00	ns
Relative BMR	0.04	-0.00	-1.12	0.297	8	0.14	ns
Altricial/precocial (dummy)	0.03	0.01	0.72	0.491	8	0.06	ns
Neonatal brain/body ratio							
Brain cube root slope	-1.47	0.10	-1.13	0.293	8	0.14	
Body cube root slope	-0.64	0.13	-3.10	0.015	8	0.55	*
Allometric RGP slope							
Brain cube root slope	-2.40	0.94	-0.66	0.530	7	0.06	ns
Body cube root slope	-1.75	1.06	-3.50	0.010	7	0.64	**

Fig. S6. Human brain growth models

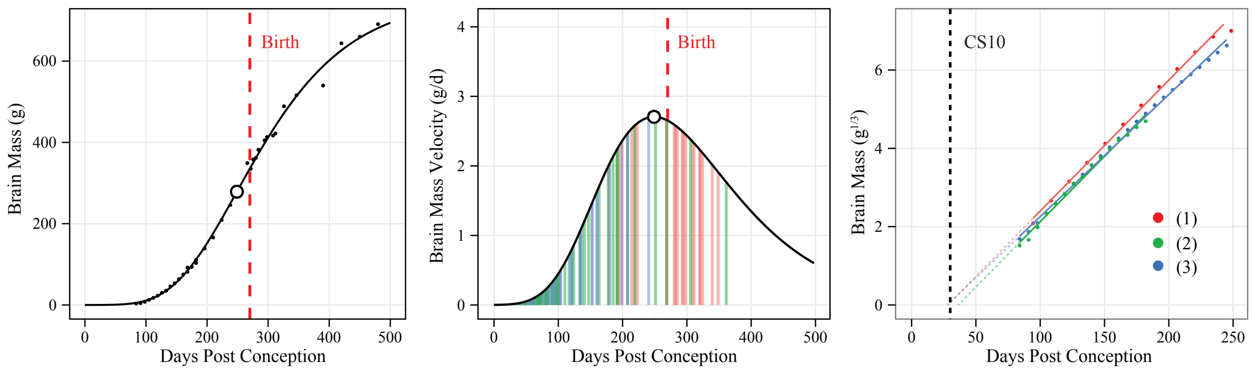

Species	*Homo sapiens*		**Peak velocity**	2.705	g/d
Gestation	270	dpc	**PV age**	248.9	dpc
Carnegie Stage 10:	29	dpc	**PV brain size**	278.7	g

Gompertz model: Singer et al., 1998; Coppoletta & Wolbach, 1933; Hansen et al., 2003

OLS regression: (dpc) predicting (brain mass [g])$^{1/3}$

	Source	*slope*	*y-int.*	*x-int.*	r^2
(1)	Guihard-Costa et al. 2002	0.0334	-0.94	28.2	1.00
(2)	Hansen et al., 2003	0.0333	-1.21	36.2	0.99
(3)	Maroun & Graem, 2005	0.0312	-0.86	27.6	1.00
	Average	**0.0327**	**-1.00**	**30.7**	**n/a**

Fig. S7. Rhesus macaque brain growth models

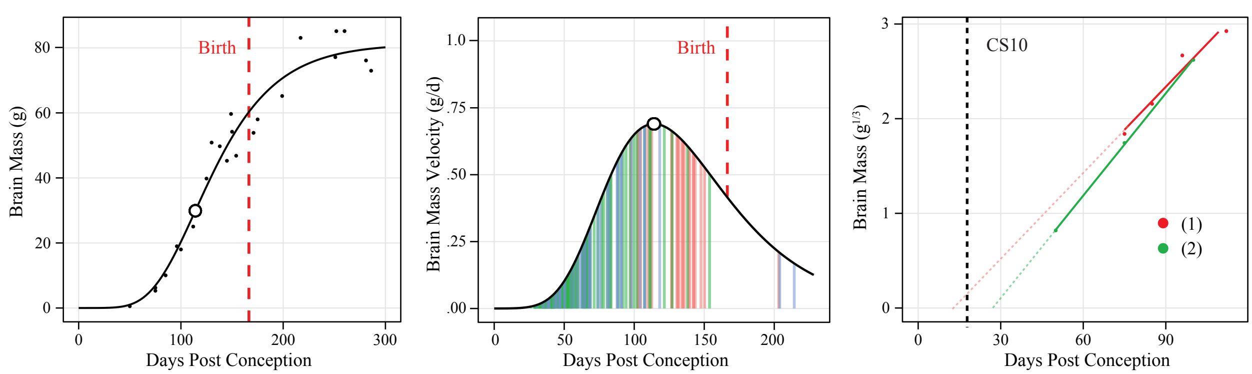

Species	*Macaca mulatta*		**Peak velocity**	0.690	g/d
Gestation	166.5	dpc	**PV age**	114.1	dpc
Carnegie Stage 10:	22	dpc	**PV brain size**	29.90	g

Gompertz model: Cheek, 1975; Kerr et al., 1974

OLS regression: (dpc) predicting (brain mass[g])$^{1/3}$

	Source	*slope*	*y-int.*	*x-int.*	r^2
(1)	Cheek, 1975	0.0303	-0.39	12.8	0.96
(2)	Kerr et al., 1974	0.0360	-0.97	27.0	1.00
	Average	**0.0331**	**-0.68**	**19.9**	**n/a**

Fig. S8. Marmoset brain growth models

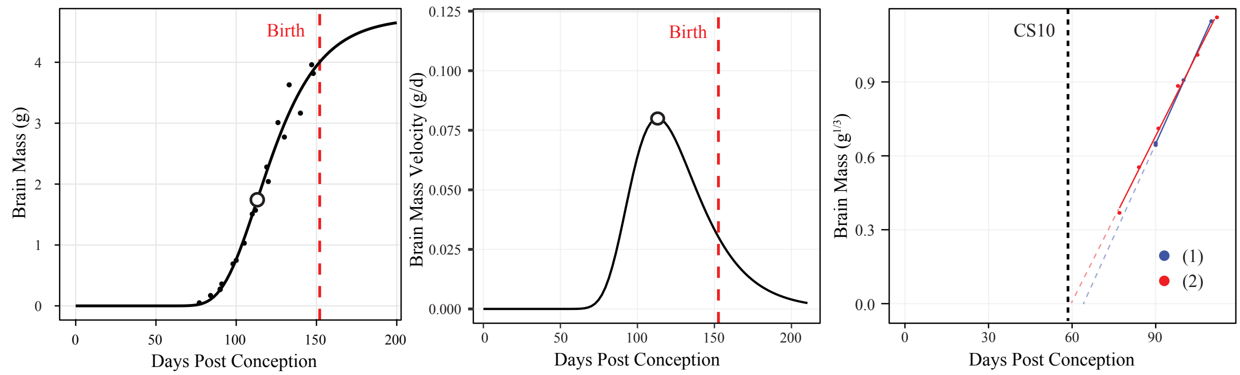

Species	*Callithrix jacchus*		**Peak velocity**	0.080	g/d
Gestation	152	dpc	**PV age**	113.1	dpc
Carnegie Stage 10*:	58.5	dpc	**PV brain size**	1.74	g

Gompertz model: Chambers & Hearn, 1985; Hikishima et al., 2012

* Estimated from Philips 1976, which gives values for CS9 (57 dpc) and CS11 (60dpc).

OLS regression: (dpc) predicting (brain mass [g])$^{1/3}$

	Source	*slope*	*y-int.*	*x-int.*	r^2
(1)	Chambers & Hearn, 1985	0.0250	-1.60	64.0	1.0
(2)	Hikishima et al., 2012	0.0220	-1.34	59.7	1.0
	Average	**0.0235**	**-1.47**	**61.9**	**n/a**

Fig. S9. Guinea pig brain growth models

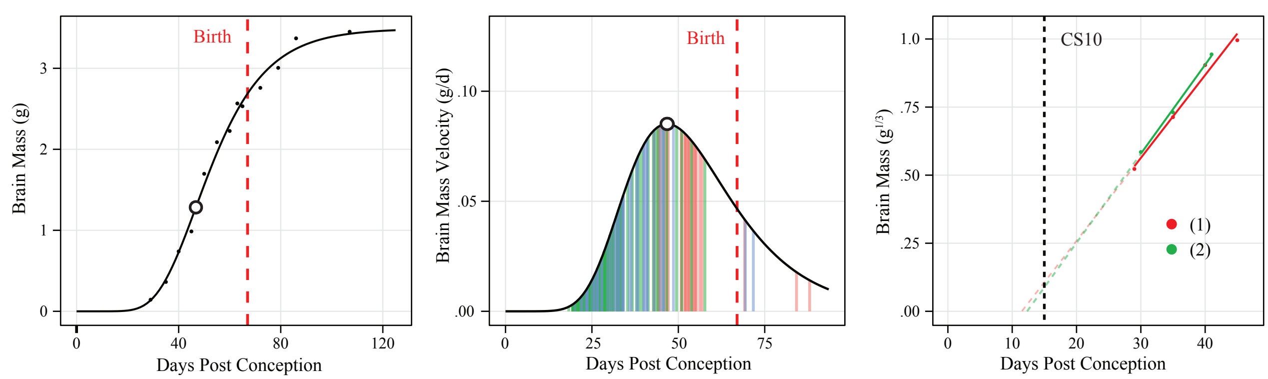

Species	*Cavia porcellus* (guinea pig)		**Peak velocity**	0.0852	g/d
Gestation	67	dpc	**PV age**	46.76	dpc
Carnegie Stage 10:	14.5	dpc	**PV brain size**	1.284	g

Gompertz model: Dobbing & Sands, 1970

OLS regression: (dpc) predicting (brain mass [g])$^{1/3}$

	Source	*slope*	*y-int.*	*x-int.*	r^2
(1)	Dobbing & Sands, 1970*	0.0304	-0.35	11.5	0.98
(2)	Edwards et al., 1976	0.0327	-0.40	12.3	1.00
	Average	**0.0316**	**-0.38**	**11.9**	**n/a**

Fig. S10. Rabbit brain growth models

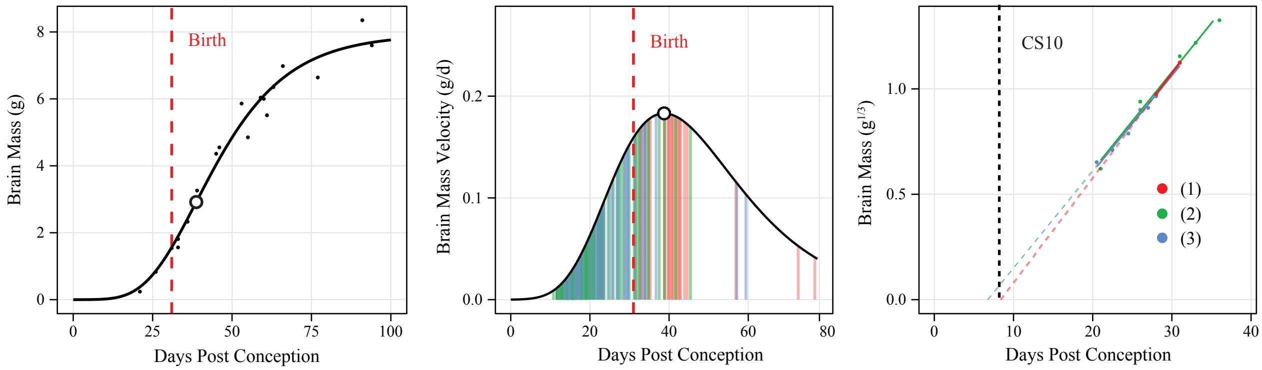

Species	*Oryctolagus cuniculus* (rabbit)		**Peak velocity**	0.183	g/d
Gestation	31	dpc	**PV age**	38.73	dpc
Carnegie Stage 10:	8.5	dpc	**PV brain size**	2.917	g

Gompertz model: Harel et al., 1972; Davison & Wadja, 1959

OLS regression: (dpc) predicting (brain mass [g])$^{1/3}$

	Source	*slope*	*y-int.*	*x-int.*	r^2
(1)	Edson et al., 1975	0.0498	-0.42	8.4	0.99
(2)	Harel et al., 1972	0.0465	-0.32	6.8	0.82
(3)	Hudson et al., 1975	0.0457	-0.31	6.7	0.99
	Average	**0.0473**	**-0.35**	**7.3**	**n/a**

Fig. S11. Rat brain growth models

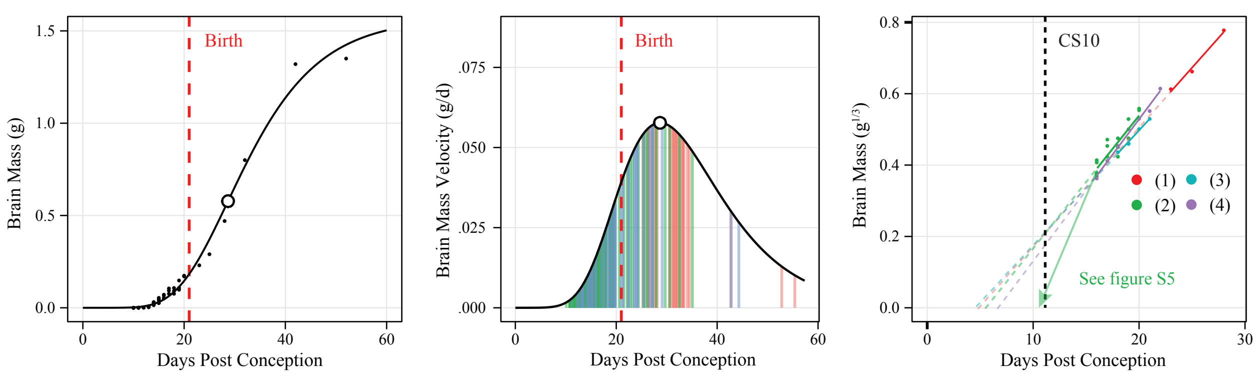

Species	*Rattus rattus* (rat)		**Peak velocity**	0.0574	g/d
Gestation	21	dpc	**PV age**	28.73	dpc
Carnegie Stage 10:	11	dpc	**PV brain size**	0.580	g

Gompertz model: Gille et al., 1996; Goedbloed, 1976

OLS regression: (dpc) predicting (brain mass [g])$^{1/3}$

	Source	*slope*	*y-int.*	*x-int.*	r^2
(1)	Gille et al., 1996	0.0334	-0.16	4.9	0.99
(2)	Goedbloed, 1976	0.0372	-0.21	5.5	0.82
(3)	Schneidereit, 1985	0.0321	-0.14	4.5	0.99
(4)	Sikov & Thomas, 1970	0.0397	-0.26	6.7	0.99
	Average	**0.0356**	**-0.68**	**5.4**	**n/a**

Fig. S12. Mouse brain growth models

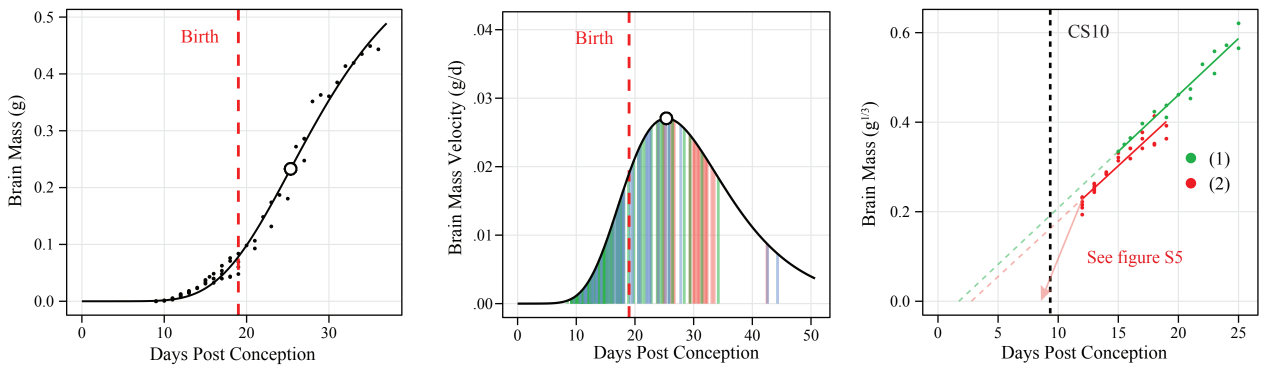

Species	*Mus musculus* (mouse)		**Peak velocity**	0.0271	g/d
Gestation	19	dpc	**PV age**	25.35	dpc
Carnegie Stage 10:	9.5	dpc	**PV brain size**	0.233	g

Gompertz model: Wingert, 1967; Goedbloed, 1976

		OLS regression: (dpc) predicting (brain mass [g])$^{1/3}$			
	Source	*slope*	*y-int.*	*x-int.*	r^2
(1)	Wingert, 1967	0.0252	-0.04	1.7	0.95
(2)	Goedbloed, 1976	0.0248	-0.07	2.8	0.91
	Average	**0.0250**	**-0.06**	**2.3**	**n/a**

Fig. S13. Ox brain growth models

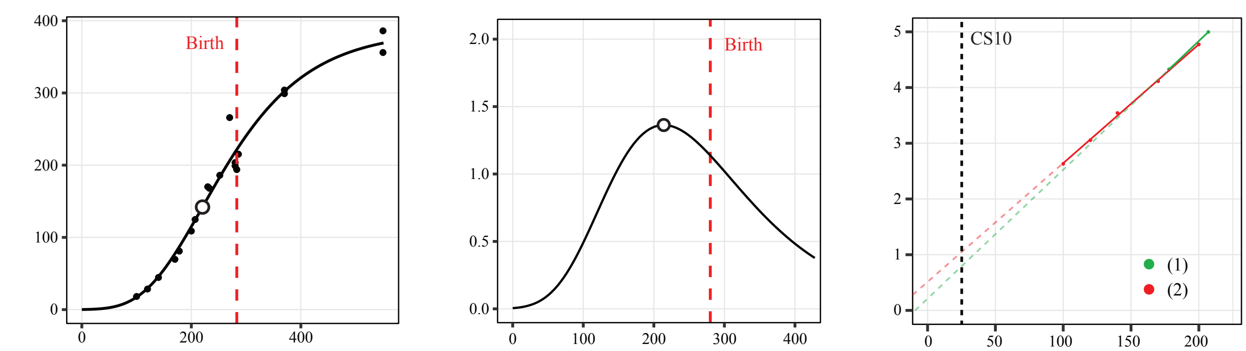

Species	*Bos taurus* (ox)		**Peak velocity**	1.3369	g/d
Gestation	280	dpc	**PV age**	220.41	dpc
Carnegie Stage 10*:	24	dpc	**PV brain size**	142.00	g

Gompertz model: Hubbert et al., 1972, Reeves et al., 1972, Crile & Quiring 1940

* Estimated by subtracting 2 days from known CS12 (26dpc; Noden, pers. comm.), the gap observed in sheep and pig.

		OLS regression: (dpc) predicting (brain mass [g])$^{1/3}$			
	Source	*slope*	*y-int.*	*x-int.*	r^2
(1)	Hubbert et al., 1972	0.0210	0.51	-24.3	1.00
(2)	Reeves et al., 1972	0.0230	0.21	-9.1	1.00
	Average	**0.0220**	**0.36**	**-16.7**	**n/a**

Fig. S14. Sheep brain growth models

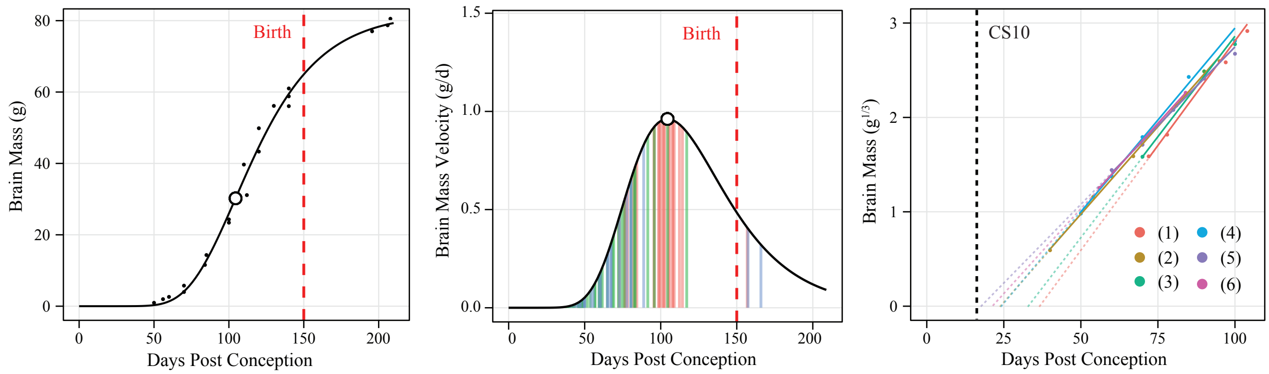

Species	*Ovis aries* (sheep)		**Peak velocity**	0.961	g/d
Gestation	150	dpc	**PV age**	104.45	dpc
Carnegie Stage 10:	16	dpc	**PV brain size**	30.22	g

Gompertz model: Rattray et al, 1975; Wallace, 1945; Richardson & Hebert, 1978; Duncan et al., 2004

OLS regression: (dpc) predicting (brain mass [g])$^{1/3}$

	Source	*slope*	*y-int.*	*x-int.*	*r^2*
(1)	Barcroft, 1946	0.0443	-1.62	36.6	1.00
(2)	McIntosh et al., 1979	0.0371	-0.88	23.7	1.00
(3)	Rattray et al., 1975	0.0426	-1.40	32.8	1.00
(4)	Richardson & Hebert, 1979	0.0390	-0.95	24.4	1.00
(5)	Thurley et al., 1973	0.0333	-0.59	17.6	1.00
(6)	Wallace, 1945	0.0360	-0.76	21.2	1.00
	Average	**0.0387**	**-1.03**	**26.1**	**n/a**

Fig. S15. Pig brain growth models

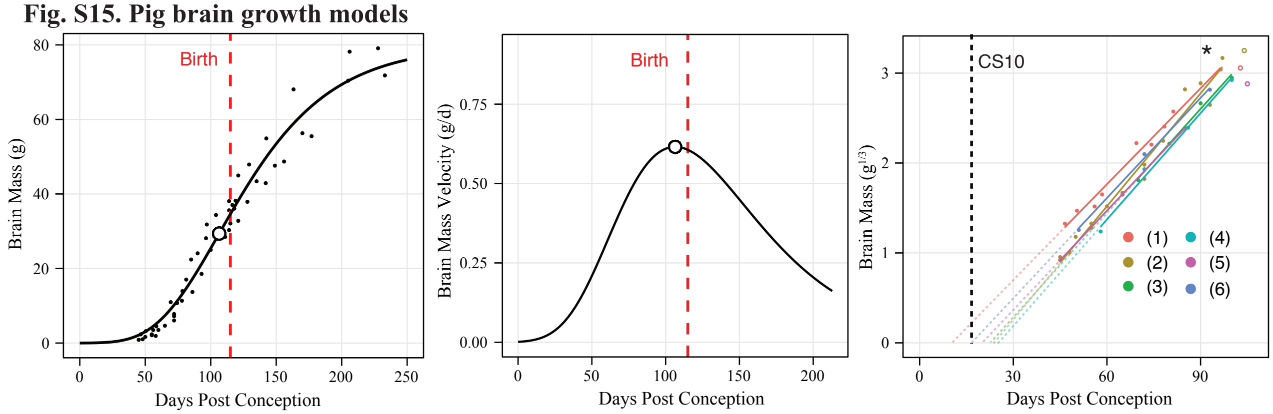

Species	*Sus scrofa* (pig)		**Peak velocity**	0.674	g/d
Gestation	150	dpc	**PV age**	111.98	dpc
Carnegie Stage 10:	16	dpc	**PV brain size**	32.86	g

Gompertz model: Dickerson & Dobbing, 1967; Done & Hebert, 1968; Tumbleson, 1973
* Three decelerated values removed from models

OLS regression: (dpc) predicting (brain mass [g])$^{1/3}$

	Source	*slope*	*y-int.*	*x-int.*	*r^2*
(1)	Dickerson & Dobbing, 1967	0.0334	-0.23	7.0	0.98
(2)	Done & Herbert, 1968	0.0412	-0.95	23.1	0.98
(3)	Pond et al., 2000	0.0386	-0.87	22.6	0.99
(4)	Tumbleson, 1973	0.0394	-0.99	25.2	0.99
(5)	Ullrey et al., 1965	0.0371	-0.62	16.6	1.00
(6)	Vallet & Freking, 2006	0.0331	-0.52	15.8	0.99
	Average	**0.0371**	**-0.70**	**18.4**	**n/a**

Fig. S16. Wallaby brain growth models

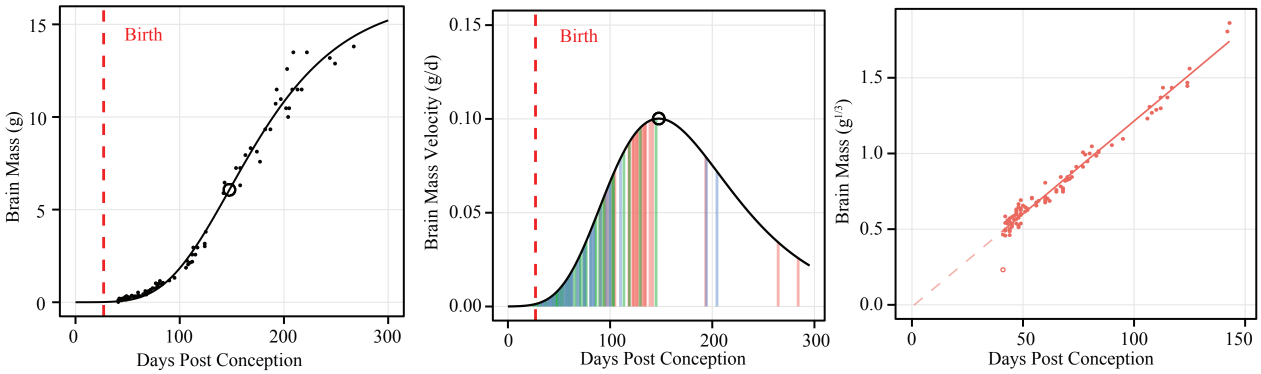

Species	*Macropus eugenii* (wallaby)	**Peak velocity**	0.100 g/d
Gestation	27 dpc	**PV age**	147.64 dpc
Carnegie Stage 10:	unknown	**PV brain size**	6.068 g

Gompertz model: Renfree et al., 1982

OLS regression: (dpc) predicting (brain mass)$^{1/3}$

	Source	*slope*	*x-int.*	*y-int.*	r^2
(1)	**Renfree et al., 1982**	**0.0123**	**-0.01**	**0.97**	**0.97**

Fig. S17. Bird and opossum brain growth models

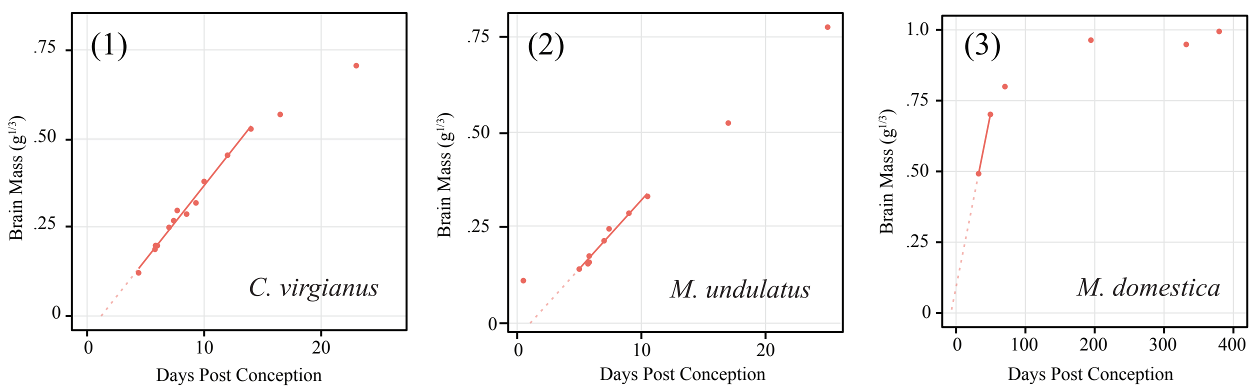

OLS regression: (dpc) predicting (brain mass)$^{1/3}$

	Source	*slope*	*x-int.*	*y-int.*	r^2
(1)	**Quail (*C. virgianus*)** Striedter & Charvet, 2008	**0.0416**	**1.20**	**-0.05**	**0.99**
(2)	**Parakeet (*M. undulatus*)** Striedter & Charvet, 2008	**0.0345**	**0.87**	**-0.03**	**0.98**
(3)	**Opossum (*M. domestica*)** Seelke et al., 2013	**0.0133**	**-4.50**	**0.06**	**n/a**

Fig. S18 Fetal body growth cube-root regression models

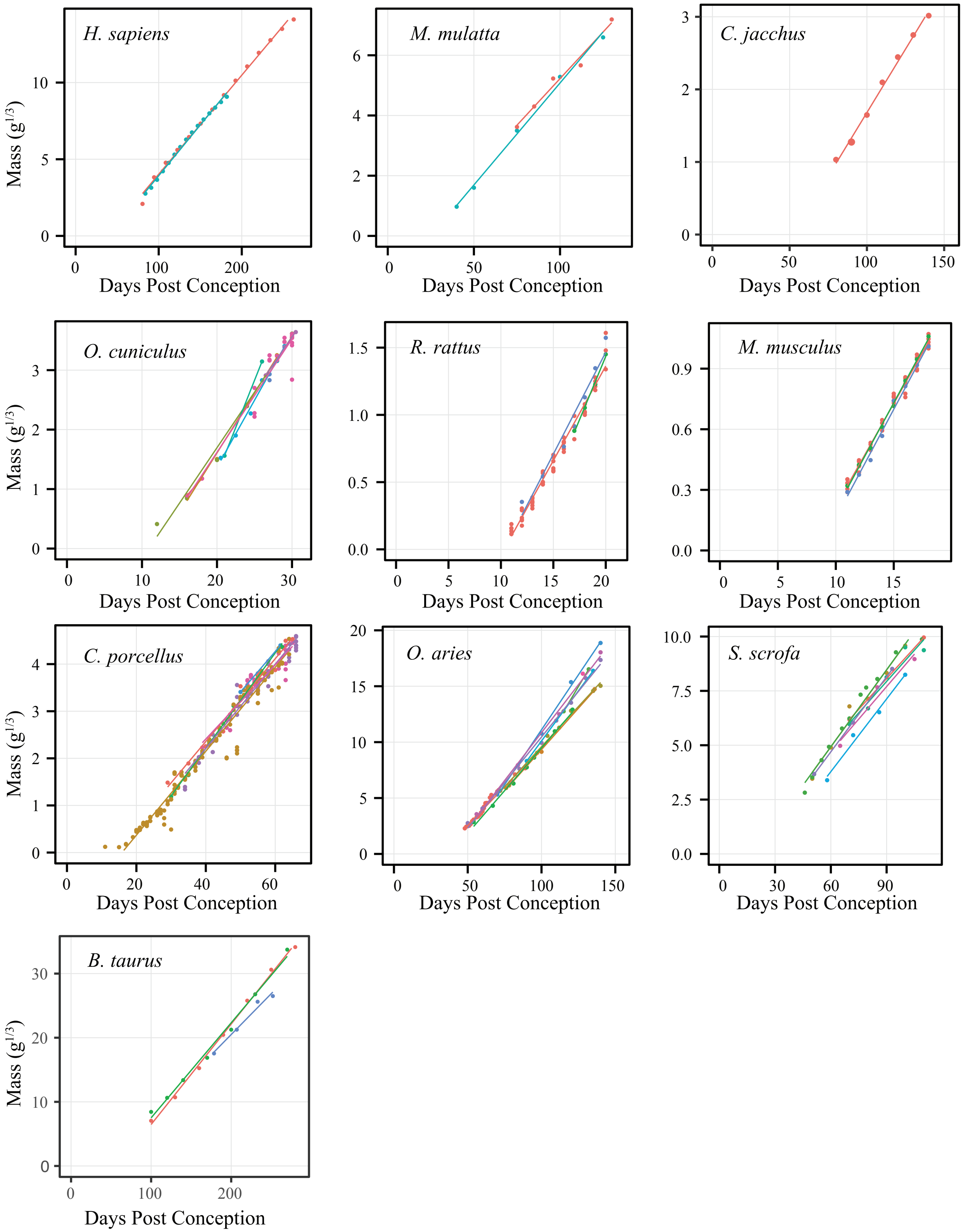

Table S8. Fetal body growth cube root models by source

Species	Source	beta	y-int.	x-int.	r^2
H. sapiens	Hansen et al., 2003	0.0661	-2.68	40.6	1.00
	Guihard-Costa et al., 2002	0.0646	-2.44	37.7	1.00
	Average	**0.0654**	**-2.56**	**39.2**	**N/A**
M. mulatta	Kerr et al., 1974	0.0678	-1.70	25.0	1.00
	Cheek, 1975	0.0619	-0.97	15.6	0.98
	Average	**0.0648**	**-1.33**	**20.3**	**N/A**
C. jacchus	**Chambers & Hearn 1985**	**0.0350**	**-1.82**	**52.0**	**0.99**
C. porcellus	Sparks et al., 1985	0.0787	-0.74	9.4	0.88
	Myers et al., 1982	0.0893	-1.36	15.2	0.95
	Lafeber et al., 1984	0.0859	-0.89	10.3	1.00
	Edwards et al., 1976	0.1012	-1.83	18.1	1.00
	Draper, 1920	0.0891	-1.41	15.9	0.96
	Dobbing & Sands, 1970*	0.0879	-1.16	13.2	0.98
	Average	**0.0887**	**-1.23**	**13.7**	**N/A**
O. cuniculus	Abdul-Karim & Bruce, 1972	0.1403	-1.35	9.6	1.00
	Bruce & Abdul-Karim, 1973	0.2013	-2.42	12.0	1.00
	Davison & Wadja, 1959	0.1866	-2.04	10.9	0.99
	Harel et al., 1972**	0.3169	-5.09	16.1	1.00
	Vidyasagar & Chernick, 1975	0.1825	-1.92	10.5	1.00
	Zilversmit et al., 1972	0.1907	-2.19	11.5	0.92
	Average	**0.1803**	**-1.98**	**10.9**	**N/A**
R. rattus	Goedbloed, 1976	0.1452	-1.53	10.5	0.97
	Schneidereit, 1985	0.1882	-2.33	12.4	1.00
	Sikov & Thomas, 1970	0.1515	-1.56	10.3	0.96
	Average	**0.1616**	**-1.80**	**11.1**	**N/A**
M. musculus	Goedbloed, 1976	0.1026	-0.81	7.9	0.99
	MacDowell et al., 1927	0.1027	-0.81	7.9	1.00
	Wingert, 1969	0.1005	-0.81	8.0	0.99
	Average	**0.1019**	**-0.81**	**7.9**	**N/A**
O. aries	Astrom, 1967	0.1389	-4.39	31.7	0.98
	Barcroft, 1946	0.1435	-4.75	33.1	1.00
	Bell et al., 1987	0.1480	-5.47	37.0	1.00
	Frasch et al., 2007	0.2213	-12.69	57.3	1.00
	McIntosh et al., 1979	0.1527	-5.79	37.9	1.00
	Osgerby et al., 2002	0.1793	-7.83	43.7	1.00
	Rattray et al., 1975	0.1964	-8.53	43.4	1.00
	Richardson & Hebert, 1978*	0.1671	-6.32	37.8	1.00
	Wallace, 1945	0.1714	-6.29	36.7	1.00
	Average	**0.1687**	**-6.90**	**39.8**	**N/A**
S. scrofa	Hard & Anderson, 1983	0.0944	-0.43	4.6	1.00
	Knight et al., 1977	0.1090	-1.38	12.6	0.97
	Marrable & Ashdown, 1967	0.1120	-1.63	14.6	0.97
	Pond et al., 2000	0.0961	-0.72	7.4	0.93
	Tumbleson, 1973	0.1029	-2.91	26.1	0.99
	Ullrey et al., 1965	0.1040	-2.21	19.2	1.00
	Vallet & Freking, 2006	0.0997	-1.28	12.8	0.96
	Average	**0.1026**	**-1.18**	**10.5**	**N/A**
B. taurus	Reeves et al. 1972	0.1274	-4.97	39.1	0.98
	Hubbert et al. 1972	0.1482	-7.32	49.4	0.99
	Ferrell et al. 1982	0.1567	-9.20	58.7	1.00
	Average	**0.1441**	**-7.16**	**49.1**	**N/A**

* Note: original data in this paper was unavailable, and was reconstructed from plots published as figures.
** Outlier excluded from the average.

Fig. S19 Fetal liver growth cube-root regression models

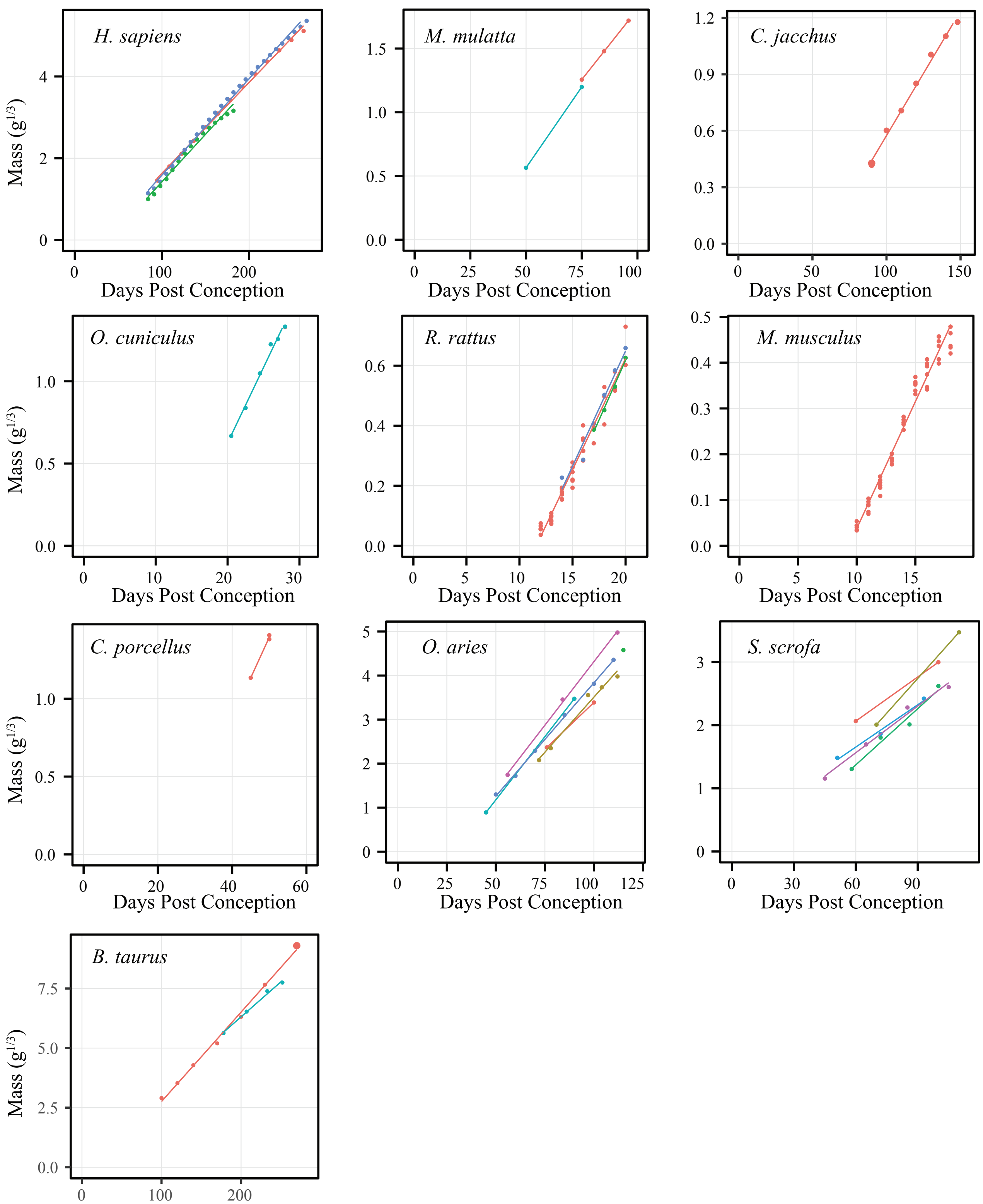

Table S9. Fetal liver growth cube root models by source

Species	Source	beta	y-int.	x-int.	R^2
H. sapiens	Guihard-Costa et al., 2002	0.0222	-0.59	26.5	1.00
	Hansen et al., 2003	0.0232	-0.90	38.6	0.99
	Maroun & Graem, 2005	0.0236	-0.77	32.7	1.00
	Average	**0.0230**	**-0.75**	**32.6**	**N/A**
M. mulatta	Cheek, 1975	0.0221	-0.40	18.1	1.00
	Kerr et al., 1974	0.0242	-0.64	26.3	1.00
	Average	**0.0231**	**-0.52**	**22.2**	**N/A**
C. jacchus	**Chambers & Hearn 1985**	**0.0132**	**-0.75**	**56.6**	**0.99**
C. porcellus	**Composite data[1]**	**0.0296**	**-0.15**	**4.9**	**0.94**
O. cuniculus	**Hudson & Hull, 1975**	**0.0917**	**-1.21**	**13.2**	**0.99**
R. rattus	Goedbloed, 1976	0.0741	-0.86	11.6	0.96
	Schneidereit, 1985	0.0796	-0.97	12.2	0.99
	Sikov & Thomas, 1970	0.0768	-0.89	11.6	0.97
	Average	**0.0768**	**-0.91**	**11.8**	**N/A**
M. musculus	**Goedbloed, 1976**	**0.0555**	**-0.52**	**9.3**	**0.97**
O. aries	Bell et al., 1987	0.0425	-0.86	20.2	1.00
	Barcroft, 1946	0.0501	-1.50	29.9	0.99
	Osgerby et al., 2002	0.0574	-1.69	29.5	1.00
	Richardson & Hebert, 1978*	0.0495	-1.18	23.8	1.00
	Wallace, 1945	0.0577	-1.45	25.2	1.00
	Average	**0.0514**	**-1.34**	**25.7**	**N/A**
S. scrofa	Hard & Anderson, 1983	0.0366	-0.55	15.1	1.00
	Hafez et al., 1958	0.0242	0.60	-24.8	1.00
	Tumbleson, 1973	0.0262	-0.16	6.0	0.96
	Ullrey et al., 1965	0.0232	0.26	-11.1	0.99
	Vallet & Freking, 2006*	0.0246	0.09	-3.5	0.99
	Average	**0.0270**	**-0.47**	**-3.7**	**N/A**
B. taurus	Reeves et al. 1972	0.0293	0.44	-15.1	0.99
	Hubbert et al. 1972	0.0375	-0.99	26.5	1.00
	Average	**0.0334**	**-0.28**	**5.8**	**N/A**

1. Data was combined from Jones & Parer, 1983, Lafeber et al., 1984, and Dwyer et al. 1995 to produce this estimate. Data from Jones & Parer was incorrectly listed in the original paper as 26.4g liver at ~34g body size; in this analysis it is corrected to 2.64g liver size at 50dpc, which is consistent with other sources.

* Note: original data in this paper was unavailable, and was reconstructed from plots published as figures.
** Note: Beta values for these studies are not included in the average, as x-intercepts indicate the onset of exponential growth prior to conception.

Fig. S20 Fetal heart growth cube-root regression models

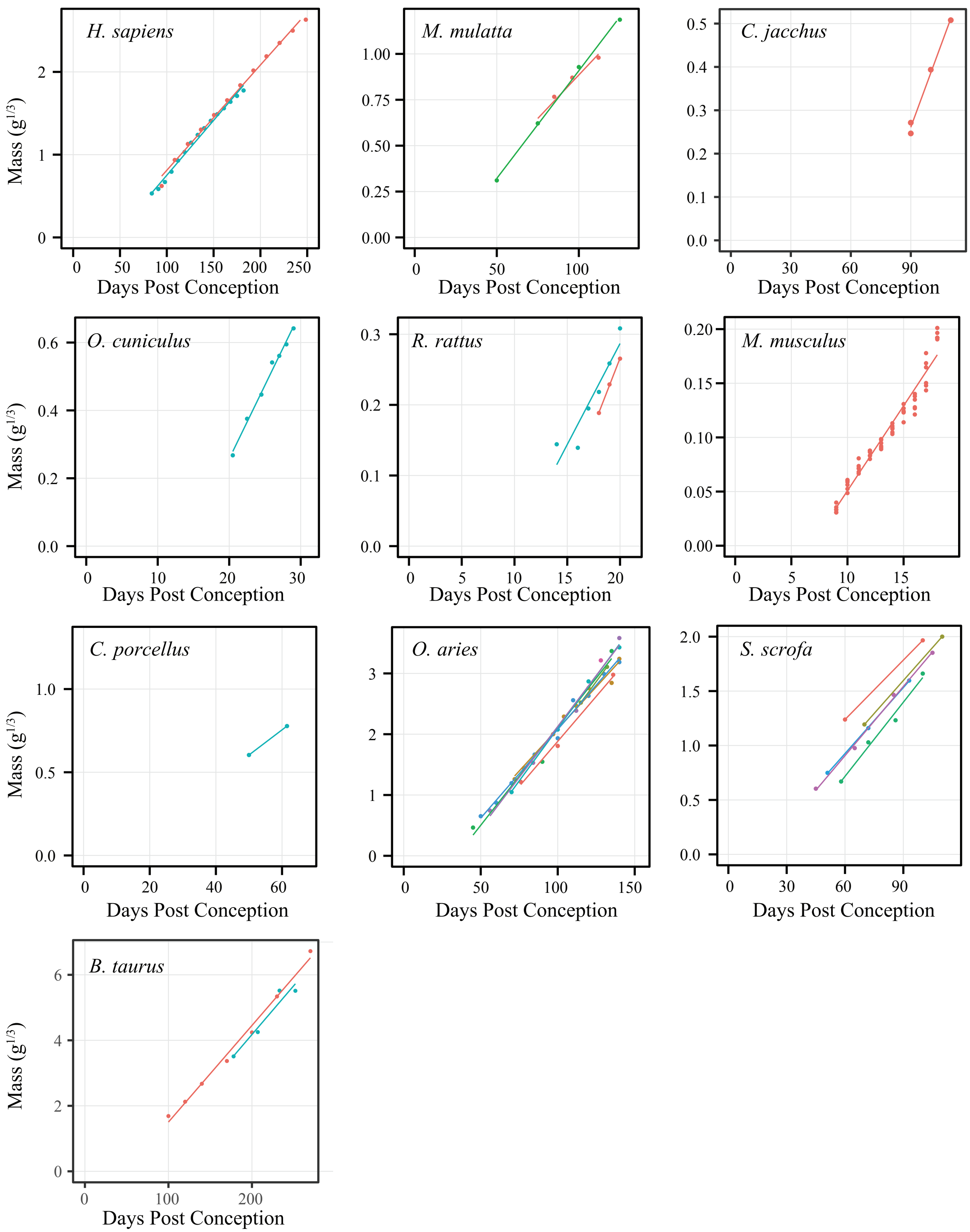

Table S10. Fetal heart growth cube root models by source

Species	Source	beta	y-int.	x-int.	R^2
H. sapiens	Guihard-Costa et al., 2002	0.0124	-0.42	33.4	0.99
	Hansen et al., 2003	0.0133	-0.57	43.4	0.99
	Average	**0.0128**	**-0.50**	**38.4**	**N/A**
M. mulatta[1]	Cheek, 1975	0.0110	-0.19	17.5	0.97
	Kerr et al., 1974	0.0117	-0.27	22.6	1.00
	Average	**0.0114**	**-0.23**	**20.0**	**N/A**
C. jacchus	**Chambers & Hearn 1985**	**0.0125**	**-0.87**	**69.2**	**0.99**
C. porcellus	**Lafeber et al., 1984**	**0.0151**	**-0.15**	**10.1**	**1.00**
O. cuniculus	**Hudson & Hull, 1975**	**0.0434**	**-0.61**	**14.1**	**0.99**
R. rattus	Schneidereit, 1985	0.0385	-0.50	13.1	1.00
	Sikov & Thomas, 1970	0.0286	-0.29	10.0	0.88
	Average	**0.0335**	**-0.40**	**11.6**	**N/A**
M. musculus	**Goedbloed, 1976**	**0.0157**	**-0.11**	**6.8**	**0.96**
O. aries	Bell et al., 1987	0.0296	-1.08	36.4	1.00
	Barcroft, 1946	0.0277	-0.68	24.6	0.98
	Frasch et al., 2007	0.0346	-1.45	42.1	1.00
	Osgerby et al., 2002	0.0323	-1.11	34.4	0.98
	Rattray et al., 1975	0.0345	-1.36	39.3	1.00
	Richardson & Hebert, 1978*	0.0292	-0.84	28.7	0.99
	Wallace, 1945	0.0335	-1.22	36.5	0.99
	Average	**0.0316**	**-1.11**	**34.6**	**N/A**
S. scrofa	Hard & Anderson, 1983	0.0202	-0.22	10.8	1.00
	Hafez et al., 1958**	0.0195	0.06	-8.1	1.00
	Tumbleson, 1973	0.0201	-0.46	22.7	0.97
	Ullrey et al., 1965	0.0186	-0.18	9.7	1.00
	Vallet & Freking, 2006	0.0212	-0.36	17.2	1.00
	Average	**0.0200**	**-0.30**	**15.1**	**N/A**
B. taurus	Reeves et al. 1972	0.0298	-1.79	59.9	0.94
	Hubbert et al. 1972	0.0295	-1.45	49.1	0.99
	Average	**0.0297**	**-1.62**	**54.5**	**N/A**

1. Data after 145dg was excluded as it had already decelerated

* Note: original data in this paper was unavailable, and was reconstructed from plots published as figures.

** Note: Beta value for this study is not included in the average, as x-intercepts indicate the onset of exponential growth prior to conception.

Fig. S21 Fetal lung growth cube-root regression models

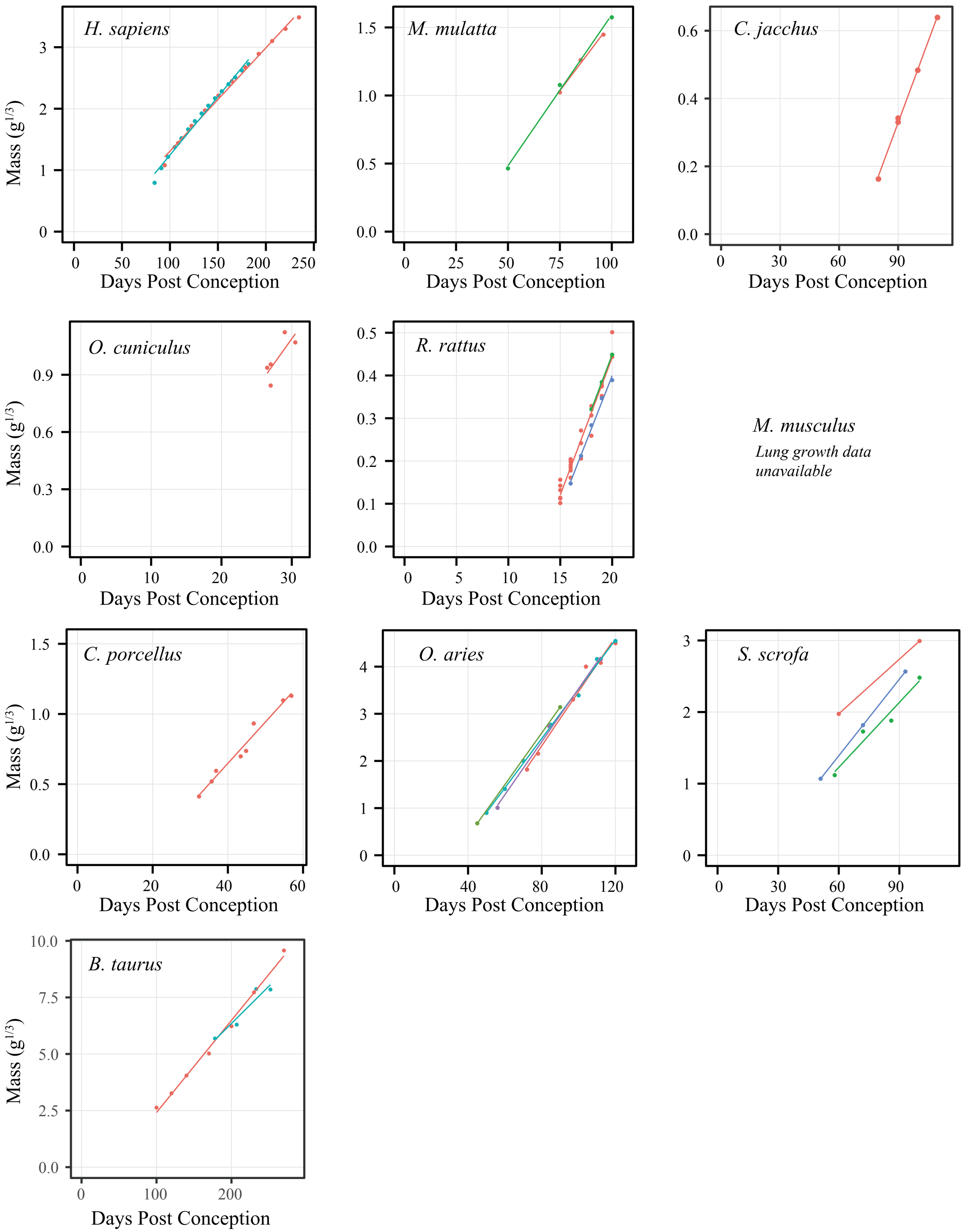

Table S11. Fetal lung growth cube root models by source

Species	Source	beta	y-int.	x-int.	R^2
H. sapiens	Guihard-Costa et al., 2002	0.0160	-0.26	16.0	0.99
	Hansen et al., 2003	0.0190	-0.65	34.3	0.99
	Average	**0.0175**	**-0.45**	**25.2**	**N/A**
M. mulatta	Cheek, 1975	0.0169	-0.21	12.6	0.99
	Kerr et al., 1974	0.0189	-0.40	21.4	0.98
	Average	**0.0179**	**-0.56**	**17.0**	**N/A**
C. jacchus	**Chambers & Hearn 1985**	**0.0157**	**-1.08**	**69.1**	**1.00**
C. porcellus	**Pasqualini et al 1976***	**0.0295**	**-0.53**	**18.0**	**0.97**
O. cuniculus	**Composite[1]**	**0.0517**	**-0.46**	**8.9**	**0.62**
R. rattus	Goedbloed, 1976	0.0604	-0.78	12.8	0.96
	Schneidereit, 1985	0.0639	-0.83	13.0	1.00
	Sikov & Thomas, 1970	0.0618	-0.84	13.5	0.99
	Average	**0.0621**	**-0.81**	**13.1**	**N/A**
O. aries	Barcroft, 1946	0.0576	-2.29	39.7	0.98
	Osgerby et al., 2002	0.0548	-1.79	32.6	1.00
	Richardson & Hebert, 1978*	0.0524	-1.71	32.7	1.00
	Wallace, 1945	0.0562	-2.09	37.2	1.00
	Average	**0.0552**	**-1.97**	**35.6**	**N/A**
S. scrofa	Hafez et al., 1958**	0.0255	0.45	-17.6	1.00
	Tumbleson, 1973	0.0303	-0.59	19.5	0.96
	Ullrey et al., 1965	0.0357	-0.75	21.0	1.00
	Average	**0.0330**	**-0.67**	**20.3**	**N/A**
B. taurus	Reeves et al. 1972	0.0329	-0.24	7.30	0.91
	Hubbert et al. 1972	0.0407	-1.66	40.7	0.99
	Average	**0.0368**	**-0.95**	**24.0**	**N/A**

1. Data was combined from Taeusch et al., 1973 and Vidyasagar & Cernick, 1975 to produce this model.

* Note: original data in this paper was unavailable, and was reconstructed from plots published as figures.

** Note: Beta value for this study is not included in the average, as x-intercepts indicate the onset of exponential growth prior to conception.

Fig. S22 Fetal kidneys growth cube-root regression models

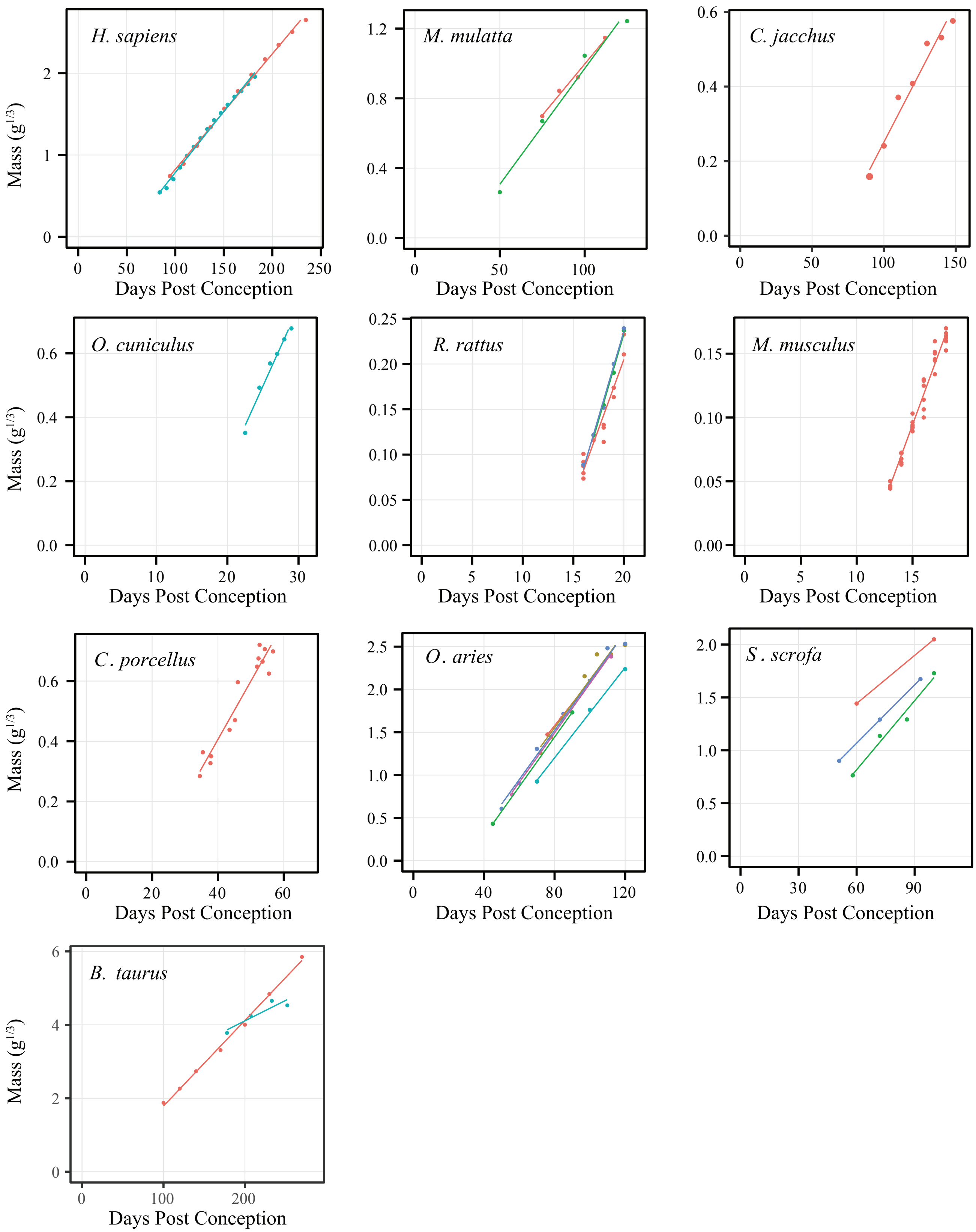

Table S12. Fetal kidney growth cube root models by source

Species	Source	beta	y-int.	x-int.	R^2
H. sapiens	Guihard-Costa et al., 2002	0.0133	-0.47	35.4	0.99
	Hansen et al., 2003	0.0150	-0.71	47.5	0.99
	Average	**0.0141**	**-0.59**	**41.5**	**N/A**
M. mulatta	Cheek, 1975	0.0118	-0.18	15.2	0.99
	Kerr et al., 1974	0.0133	-0.36	26.9	0.98
	Average	**0.0125**	**-0.27**	**21.0**	**N/A**
C. jacchus	**Chambers & Hearn 1985**	**0.0074**	**-0.49**	**66.3**	**0.97**
C. porcellus	**Pasqualini et al 1976***	**0.0194**	**-0.37**	**19.0**	**0.92**
O. cuniculus	**Hudson & Hull, 1975**	**0.0493**	**-0.73**	**14.9**	**0.98**
R. rattus	Goedbloed, 1976	0.0307	-0.41	13.3	0.92
	Schneidereit, 1985	0.0382	-0.53	13.9	0.99
	Sikov & Thomas, 1970	0.0379	-0.52	13.8	0.99
	Average	**0.0356**	**-0.49**	**13.7**	**N/A**
M. musculus	**Goedbloed, 1976**	**0.0225**	**-0.24**	**10.7**	**0.97**
O. aries	Bell et al., 1987	0.0259	-0.50	19.1	1.00
	Barcroft, 1946	0.0280	-0.69	24.5	0.94
	Osgerby et al., 2002	0.0289	-0.87	30.1	1.00
	Rattray et al., 1975	0.0264	-0.91	34.5	1.00
	Richardson & Hebert, 1978*	0.0286	-0.77	26.9	0.99
	Wallace, 1945	0.0288	-0.81	28.2	1.00
	Average	**0.0278**	**-0.76**	**27.2**	**N/A**
S. scrofa	Hafez et al., 1958**	0.0152	0.53	-35.1	1.00
	Tumbleson, 1973	0.0218	-0.49	22.6	0.97
	Ullrey et al., 1965	0.0184	-0.04	2.0	1.00
	Average	**0.0201**	**-0.26**	**12.3**	**N/A**
B. taurus	Reeves et al. 1972	**0.0111**	**1.88**	**-169.2**	**0.85**
	Hubbert et al. 1972	**0.0233**	**-0.55**	**23.4**	**1.00**
	Average	**0.0172**	**0.67**	**-72.9**	**N/A**

* Note: original data in this paper was unavailable, and was reconstructed from plots published as figures.

** Note: Beta value for this study is not included in the average, as x-intercepts indicate the onset of exponential growth prior to conception.

SI & Data Source References

Abdul-Karim RW, Bruce NW (1972) The regulatory effect of oestrogens on fetal growth: II. Uterine and placental blood flow in rabbits. *J. Reprod. Fert.* **30**, 477–480.

Åström K-E. 1967 On the early development of the isocortex in fetal sheep. *Prog. Brain Res.* **26**, 1–59.

Barcroft J. 1947 *Researches on Pre-natal Life.* Hoboken: Blackwell.

Bell AW, Battaglia FC, Meschia G. 1987 Relation between metabolic rate and body size in the ovine fetus. *J. Nutr.* **117**, 1181–1186.

Bruce NW, Abdul-Karim RW. 1973 Relationships between fetal weight, placental weight and maternal placental circulation in the rabbit at different stages of gestation. *J. Reprod. Fert.* **32**, 15–24.

Chambers PL, Hearn J. 1985 Embryonic, foetal and placental development in the Common marmoset monkey (Callithrix jacchus). *J. Zool. Lond. A* **207**, 545–561.

Cheek DB. 1975 Appendix II: Data on normal fetal and postnatal Macaca mulatta. In *Fetal and Postnatal Cellular Growth* (ed DB Cheek), pp 521–534. Hoboken, NJ: Wiley

Coppoletta JM, Wolbach SB. 1933 Body lengths and organ weights of infants and children: A study of the body length and normal weights of the more important vital organs of the body between birth and twelve years of age. *Am. J. Pathol.* **9**, 55–70.

Davison AN, Wajda M. 1959 Metabolism of myelin lipids: Estimation and separation of brain lipids in the developing rabbit. *J. Neurochem.* **4**, 353–359.

Dickerson JWT, Dobbing J. 1967 Prenatal and postnatal growth and development of the central nervous system of the pig. *Proc. R. Soc. Lond. B Biol. Sci.* **166**, 384–395.

Done JT, Hebert CN. 1968 The growth of the cerebellum in the foetal pig. *Res. Vet. Sci.* **9**, 143–148.

Draper RL. 1920 The prenatal growth of the guinea-pig. *Anat. Rec.* **18**, 369–392.

Dwyer CM, Madgwick AJA, Ward SS, Stickland NC. 1995 Effect of maternal undernutrition in early gestation on development of fetal myfibres in the guinea-pig. *Reprod. Fertil. Dev.* **7**, 1285–1292.

Edson JL, Hudson DG, Hull D. 1975 Evidence for increased fatty acid transfer across the placenta during maternal fast in rabbits. *Biol. Neonate* **27**, 50–55.

Edwards MJ, Wanner RA, Mulley RC. 1976 Growth and development of the brain in normal and heat-retarded guinea-pigs. *Neuropathol. Appl. Neurobiol.* **2**, 439–450.

Frasch MG, Müller T, Wicher C, Weiss C, Löhle M, Schwab K, Schubert H, Nathanielsz PW, Witte OW, Schwab M. 2007 Fetal body weight and the development of the control of the cardiovascular system in fetal sheep. *J. Physiol.* **579**, 893–907.

Guihard-Costa A-M, Ménez F, Delezoide A-L. 2002 Organ weights in human fetuses after formalin fixation: Standards by gestational age and body weight. *Pediatr. Dev. Pathol.* **5**, 559–578.

Ferrell CL, Laster DB, Prior RL. 1982 Mineral accretion during prenatal growth of cattle. *J. Anim. Sci.* **54**, 618–624.

Hansen K, Sung CJ, Huang C, Pinar H, Singer DB, Oyer CE. 2003 Reference values for second trimester fetal and neonatal organ weights and measurements. *Pediatr. Dev. Pathol.* **6**, 160–167.

Hard DL, Anderson LL. 1983 Nucleic acid content and growth of fetal brain, liver, and heart during inanitation in pigs. *Biol. Reprod.* **29**, 799–804.

Harel S, Watanabe K, Linke I, Schain RJ. 1972 Growth and development of the rabbit brain. *Biol. Neonate* **21**, 381–399.

Hikishima K, Sawada K, Murayama AY, Komaki Y, Kawai K, Sato N, Inoue T, Itoh T, Momoshima S, Iriki A et al. 2013 Atlas of the developing brain of the marmoset monkey constructed using magnetic resonance histology. *Neurosci.* **230**, 102–113.

Hubbert WT, Stalheim OHV, Booth GD. 1972 Changes in organ weights and fluid volumes during growth of the bovine fetus. *Growth* **36**, 217–233.

Hudson DG, Hull D. 1975 Growth of adipose tissue in the fetal rabbit. *Biol. Neonate* **27**, 71–79.

Jones CT, Parer JT. 1983 The effect of alterations in placental blood flow on the growth and nutrient supply to the fetal guinea-pig. *J. Physiol.* **343**, 525–537.

Kerr GR, Allen JR, Scheffler G, Couture J. 1974 Fetal and postnatal growth of rhesus monkeys (M. mulatta). *J. Med. Primatol.* **3**, 221–235.

Knight JW, Bazer FW, Thatcher WW, Franke DE, Wallace HD. 1977 Conceptus development in intact and unilaterally hysterectomized-ovariectomized gilts: Interrelations among hormonal status, placental development, fetal fluids and fetal growth. *J. Anim. Sci.* **44**, 620–637.

Lafeber HN, Rolph TP, Jones CT. 1984 Studies on the growth of the fetal guinea pig: The effects of ligation of the uterine artery on organ growth and development. *J. Dev. Physiol.* **6**, 441–459.

MacDowell EC, Allen E, MacDowell CG. 1927 The prenatal growth of the mouse. *J. Gen. Physiol.* **11**, 57–70.

Maroun LL, Graem N. 2005 Autopsy standards of body parameters and fresh organ weights in nonmacerated and macerated human fetuses. *Pediatr. Dev. Pathol.* **8**, 204–217.

Marrable AW, Ashdown RR. 1967 Quantitative observations on pig embryos of known ages. *J. Agr. Sci. Camb.* **69**, 443–447.

McIntosh GH, Baghurst KI, Potter BJ, Hetzel BS. 1979 Foetal brain development in the sheep. *Neuropathol. Appl. Neurobiol.* **5**, 103–114.

Myers RE, Hill DE, Holt AB, Scott RE, Mellits ED, Cheek DB. 1971 Fetal growth retardation produced by experimental placental insufficiency in the rhesus monkey. I. Body weight, organ size. *Biol. Neonate* **18**, 379–394.

Myers SA, Sparks JW, Makawski EL, Meschia G, Battaglia FC. 1982 Relationship between placental blood flow and placental and fetal size in guinea pig. *Am. J. Physiol.* **243**, H404-409.

Osgerby JC, Wathes DC, Howard D, Gadd TS. 2002 The effect of maternal undernutrition on ovine fetal growth. *J. Endocrinol.* **173**, 131–141.

Pasqualani JR, Sumida C, Gelly C, Nguyen BL. 1976 Specific [3H]-estradiol binding in the fetal uterus and testis of guinea pig: Quantitative evolution of [3H]-estradiol receptors in the differential fetal tissues (kidney, lung, uterus and testis) during fetal development. *J. Steroid Biochem.* **7**, 1031–1038.

Pond WG, Boleman SL, Fiorotto ML, Ho H, Knabe DA, Mersmann HJ, Savell JW, Su DR. 2000 Perinatal ontogeny of brain growth in the domestic pig. *Exp. Biol. Med.* **223**, 102–108.

Rattray PV, Robinson DW, Garrett WN, Ashmore RC. 1975 Cellular changes in the tissues of lambs during fetal growth. *J. Anim. Sci.* **40**, 783–788.

Reeves JT, Daoud FS, Gentry M. 1972 Growth of the fetal calf and its arterial pressure, blood gases, and hematologic data. *J. Appl. Physiol.* **32**, 240–244.

Richardson C, Hebert CN. 1978 Growth rates and patterns of organs and tissues in the ovine foetus. *Br. Vet. J.* **134**, 181–189.

Schneidereit M. 1985 Study of fetal organ growth in Wistar rats from day 17 to 21. *Lab. Anim.* **19**, 240–244.

Sikov MR, Thomas JM. 1970 Prenatal growth of the rat. *Growth* **34**, 1–14.

Singer D, Sung C, Wigglesworth J. 1991 Fetal growth and maturation: With standards for body and organ development. *Textb. Fetal Perinat. Pathol.* **1**, 11–15.

Sparks JW, Girard JR, Callikan S, Battaglia FC. 1985 Growth of fetal guinea pig: Physical and chemical characteristics. *Am. J. Physiol.* **248**, E132–139.

Taeusch HW, Carson SH, Wang NS, Avery ME. 1973 Heroin induction of lung maturation and growth retardation in fetal rabbits. *Semin. Fetal Neonatal Med.* **82**, 869–875.

Takahashi T, Nowakowski RS, Caviness VS. 1995 The cell cycle of the pseudostratified ventricular epithelium of the embryonic murine cerebral wall. *J. Neurosci.* **15**, 6046–6057.

Thurley DC, Revfeim KJA, Wilson DA. 1973 Growth of the Romney sheep foetus. *New Zeal. J. Agr. Res.* **16**, 111–114.

Tumbleson ME. 1973 Brain weight, as a function of age, in miniature swine. *Growth* **37**, 13–17.

Ullrey DE, Sprague JI, Becker DE, Miller ER. 1965 Growth of the swine fetus. *J. Anim. Sci.* **24**, 711–

717.

Vallet JL, Freking BA. 2006 Changes in fetal organ weights during gestation after selection for ovulation rate and uterine capacity in swine. *J. Anim. Sci.* **84**, 2338–2345.

Vidyasagar D, Chernick V. 1975 Effect of metopirone on the synthesis of lung surfactant in does and fetal rabbits. *Biol. Neonate* **27**, 1–16.

Waechter RV, Jaensch B. 1972 Generation times of the matrix cells during embryonic brain development: An autoradiographic study in rats. *Brain Res.* **46**, 235–250.

Wallace L. 1945 The composition of sheep foetuses. *J. Physiol.* **104S**, 33P–34P.

Wilson JG, Fradkin R, Hardman A. 1970 Breeding and pregnancy in rhesus monkeys used for teratological testing. *Teratology* **3**, 59–71.

Wingert F. 1969 Biometrische Analyse der Wachstumsfunktionen von Hirnteilen und Körpergewicht der Albinomaus. *J. Hirnforschungen* **11**, 133–197.

Zilversmit DB, Remington M, Hughes LB. 1972 Fetal growth and placental permeability in rabbits fed cholesterol. *J. Nutrition* **102**, 1681–1688.